

POST-TENSIONED CONNECTION SYSTEMS FOR SEISMIC-RESISTANT STEEL FRAMES

A.1. Introduction

The failure of welded connections in steel moment frames during recent earthquakes has led to a renewed interest in bolted connections for seismic zones. While bolted connections eliminated the difficulties associated with welding, and can provide large plastic deformation capacities within detail material C. such as angles, several major deficiencies exist in such structural systems. These deficiencies include low service level stiffness, pinched behavior due to permanent deformation of detail material, and fasteners without any significant deformation capacity. The latter point has significance in that large prying forces can develop in connections, leading to overstressing of the fasteners. Either a non-ductile fastener failure or simply loss of energy-dissipating efficiency can occur due to loss of preload. One solution is to replace individual fasteners on each face of the column with a post-tensioning element across the face of the column. This paper describes such a post-tensioned connection system under development and the results of analytical and experimental studies.

A.1.a. Post-Tensioned Connection System Concept

The intent of the post-tensioned connector system is to provide the high initial rotational stiffness of welded full-moment connections, the reliable ductility of semi-rigid connections, and the self-centering capabilities of prestressed construction. The system utilizes steel connectors and special post-tensioning elements. The post-tensioning gage length across the connection is relatively short thus a special post-tensioning material is required. Several high-strength low-modulus materials have been evaluated for the post-tensioning element including aluminum, titanium and fiber-reinforced composites. Thus far, the superelastic properties of the shape memory alloy, Nitinol, have provided the optimal solution.

The post-tensioned connection system is comprised of mild-steel beam flange connectors post-tensioned across the column face by post-tensioning elements (See Figure 17).

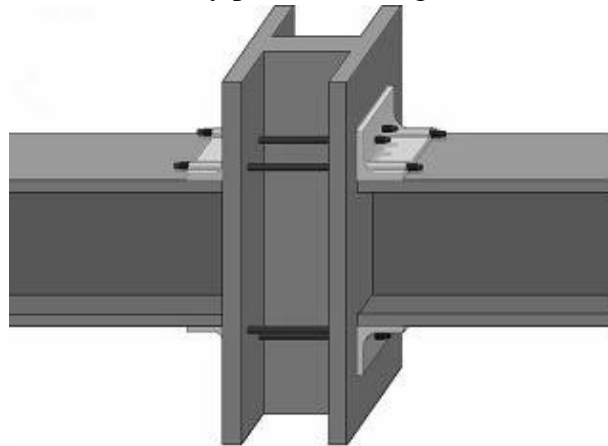


Figure 17. Schematic of Post-Tensioned Connecting System.

The connectors serve two purposes: (1) They serve as a reaction block for the post-tensioning; and (2) They provide supplemental stiffness, strength and energy dissipation to the connection system. The post-tensioning strands/bars extend across the depth of the column and twice the length of the connectors (L_{PT}). This span is several times the typical bolt grip, but an order of magnitude lower than the post-tensioning spans common in civil structures. For this reason, steel, even in its high strength forms, may not be the most efficient material for the post-tensioning strands. For this reason, a number of forms of superelastic material were evaluated, including with and without significant hysteretic capabilities. Thus, the connecting element can be designed solely as a post-tensioning element, or primarily as a dissipator, or a combination of both.

Figure 18 shows the stress-strain curves for the two types of superelastic materials evaluated in the study. Both are from the family of nickel-titanium shape-memory alloys known commonly as Nitinol. In its shape memory application, crossing of a transformation temperature causes the reverting of the material from an austenitic phase to a martensitic phase, and in this act

the reversing of permanent shape deformation termed twinning. In its superelastic application, this detwinning is accomplished through stress-inducing a stable form martensite [Duerig et al, 1990]. This behavior is obtained provided the operating temperature range is above the superelastic transition temperature. Fortunately, available transition temperatures from the various manufacturing Nitinol processes cover a wide range.

The transition temperatures for transforming between the austenitic phase and martensitic phase do not coincide with the reverse process. Thus, a hysteresis is realized in the process of stress-inducing superelastic behavior (See Fig. 19a). Typical values of the key material properties identified in the figure are listed in Table 1. In an alternate cold-worked form.

Nitinol exhibits nearly hysteresis-free behavior (See Fig. 19b). Nitinol can exhibit this linear superelastic behavior to strains up to and 4%. Table 2 gives typical properties for linear superelastic Nitinol (LSNiTi) as indicated in Figure 2b.

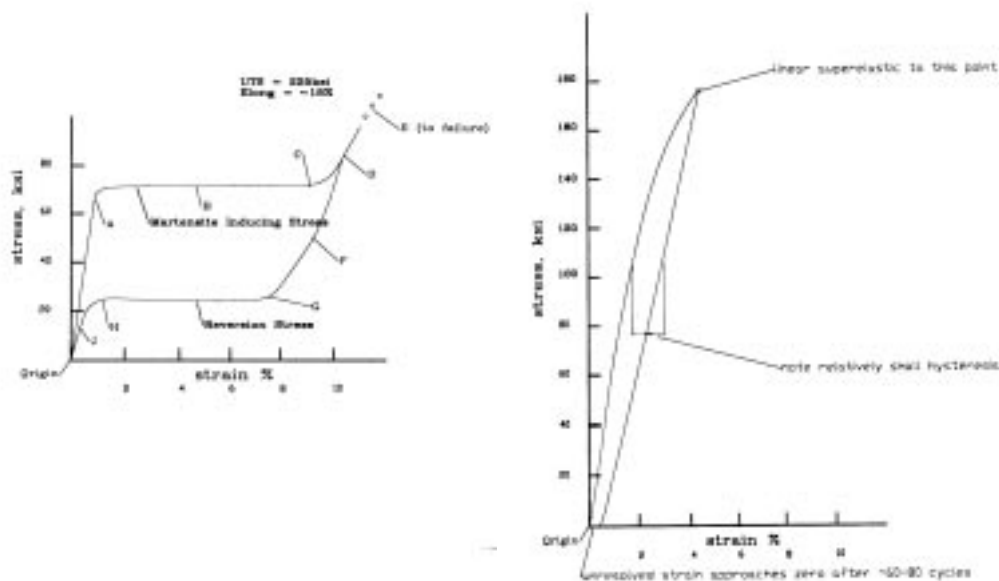


Figure 18 Nitinol Stress-Strain Characteristics: (a) Superelastic (b) Linear Superelastic.

A.1.b. Design Parameters Details

The connecting system is being developed within a performance-based engineering framework to meet requirements related to structural damage and drift. For service wind loading or low-level seismic events, the connectors are detailed to possess high inherent elastic stiffness in comparison to traditional semi-rigid connections, rendering the structural drifts within acceptable limits.

At design earthquake levels, the connectors provide stable hysteretic behavior while incurring only modest damage due to the elastic nature of the post-tensioning. For survival level events, the post-tensioning enters its superelastic ranges reducing the permanent drift in the frame.

The primary parameters controlling the behavior of the post-tensioned connecting system are: (1) the ratio of mild steel connector strength to overall strength; (2) the level of pre-tension in the tendons, (3) the length of the post-tension tendons. The development of the connecting system is driven by a performance-based design approach. Figure 19 shows a schematic indicating the regions of behavior provided by the connection.

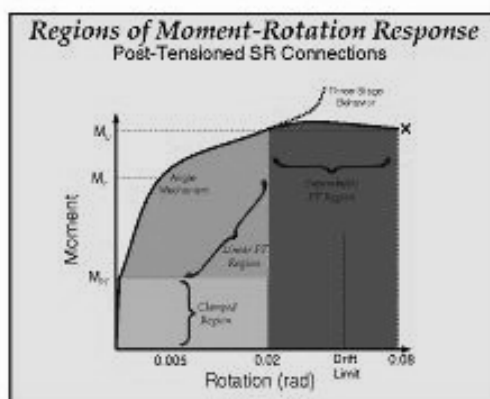


Figure 19. Schematic of Behavior Regions for PTC.

A.c.2. Analytical Program

Finite element analyses are being performed to examine the hysteretic behavior of the post-tensioned system. Parameters include location (vertical) of the post-tensioning element, pre-tension level, and the relative strength of the post-tensioning to the connector. A prototype design has been developed.

Currently, nonlinear dynamic analyses of structures employing the prototype design are being performed. The objective of these analyses is to provide system designs that meet accepted performance criteria for multiple levels of seismic intensity. The system has shown promising response reduction and self-centering effects.

A.2.a. Analytical Models:

Connection Model: A two-dimensional plane-strain finite element model was created to evaluate the hysteretic characteristics of the post-tensioned connector. Figure 20 shows a schematic of the model. The model employs one-dimensional line-type beam elements to model the beam and column. The mild connectors, in this case flange angles, are modeled using plane-strain solid elements. The degree-of-freedom (DOFs) at the ends of the angles are constrained to the beam elements to obtain the appropriate kinematic relationships required by compatibility. Contact pseudo-elements are provided between the angle elements and slaved boundaries representing the contact surface on the column flange to provide the compression zone created by the post-tensioning. Figure 21 shows hysteresis curves for the connection.

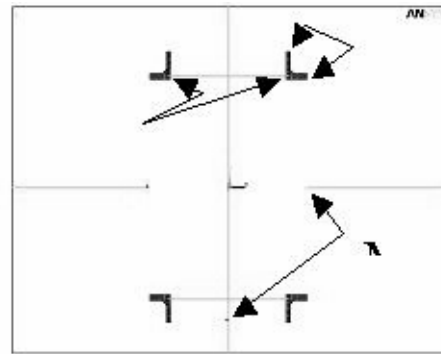


Figure 20. Schematic of 2D FE Model of PTC.

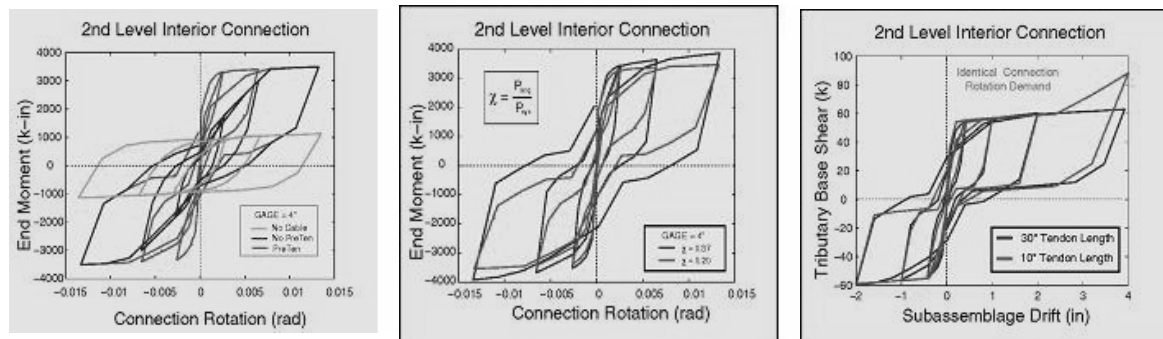


Figure 21. Moment-Rotation Characteristics of PT System: (a) Level of PT; (b) PT/Mild ratio; (c) PT Length.

Structural Model: Based on the hysteretic characteristics provided in the finite element analyses, a simpler representation was created in DRAIN-2DX to examine the connection system's performance under seismic demands. The connection is modeled as translational springs slaved to the beam-column elements similar to the FE model. A pair of springs, one ideal elastoplastic and one slip-type behavior were used to reproduce the pinched hysteresis of bolted semi-rigid connection. The flag-shaped hysteresis of the superelastic tendons were obtained by two elements: an elastoplastic translational spring in parallel with a linearly superelastic truss element.

A.2.b. Analytical Program

A three-story LA structure developed for the SAC program was used as the prototype frame. A second, six-story frame of the same plan and floor loading was designed to meet the 1997 UBC. The contribution of the floor slab to the bare frame was ignored in the representation of the structure. The first set of records were performed on a full frame. These results were compared to the results of a single column line (a multi-story sub-assembly). The results were reasonably close, indicating that overturning effects in the structure and axial force effects in the connecting system were not significant. Therefore, the large parametric studies were performed on the multi-story assemblage. The SAC ground motions were used in the evaluations.

A.3. Prototype Development and Experimental Program

A.3.a. Alpha Prototype Experiment

Meetings were held with industry partners to develop the prototype. Subsequently, a Nitinol strand configuration was devised that meets the specifications of the prototype design. At this time, the proper end-anchorage detail is being investigated. An experimental setup has been designed and built to test the post-tensioned connection system. The experiments occurred following the anchorage design is complete.



Figure22.



Figure23.



Figure24.



Figure25.

B. Findings from Post-Tensioned Connector Research

B.1. Analytical Results

The following pages show analytical results from nonlinear dynamic analyses of structures containing the PT Connection system.

B.1.a General Behavior

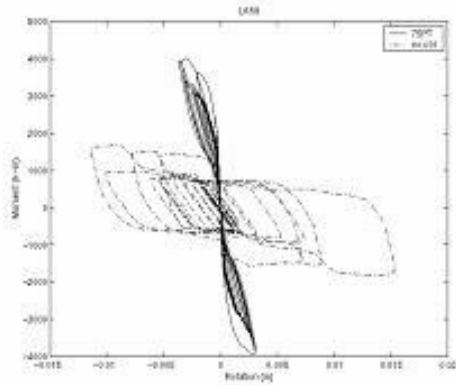


Figure 22.

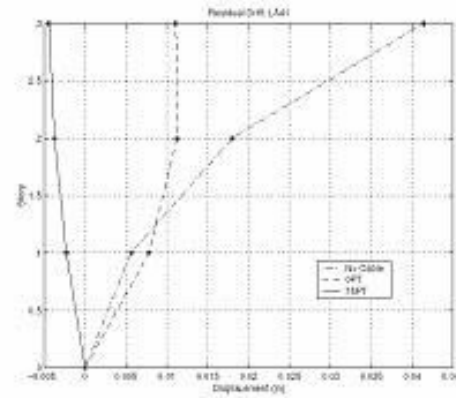


Figure 23.

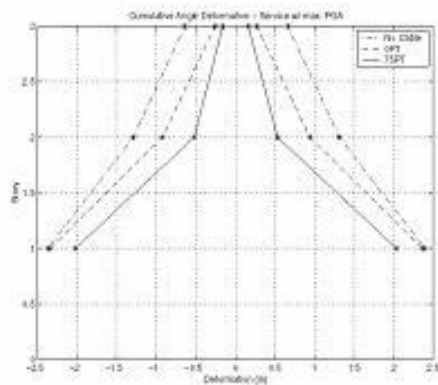


Figure 24.

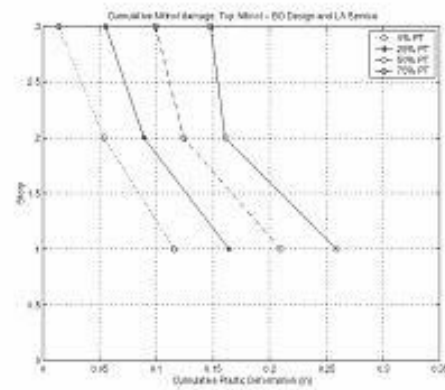
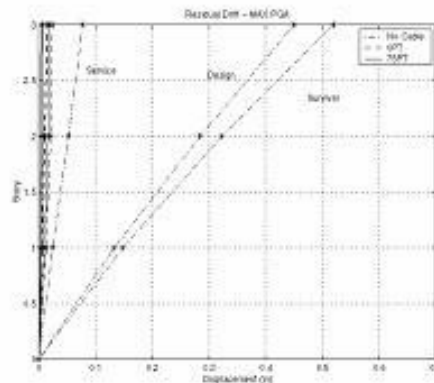
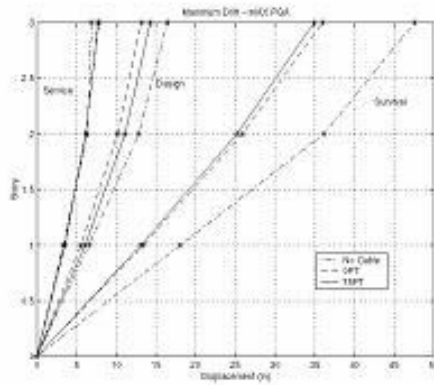


Figure 25.

Overall Response:



B.1.b. PT Tendon Material

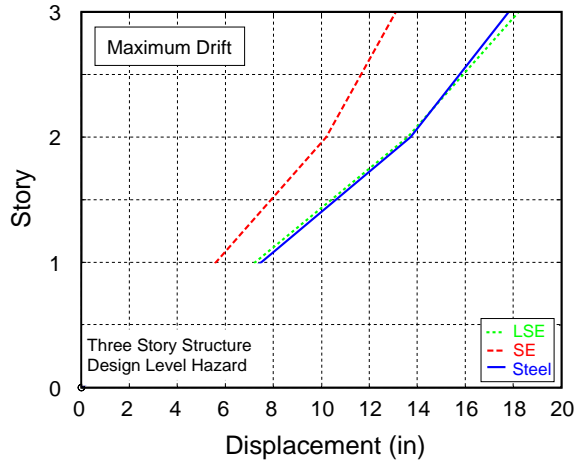


Figure 28.

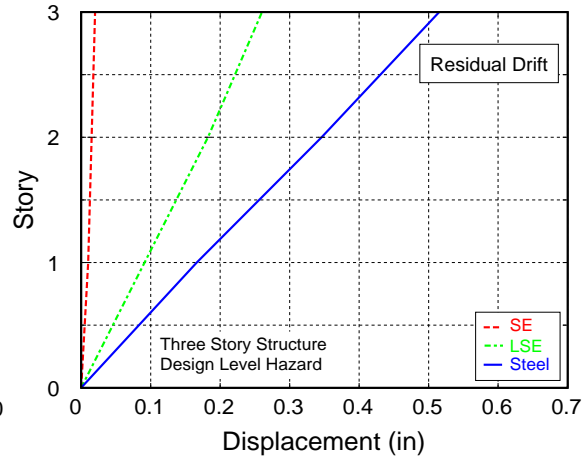


Figure 29.

Comparison: Steel, SE Nitinol; LSE Nitinol

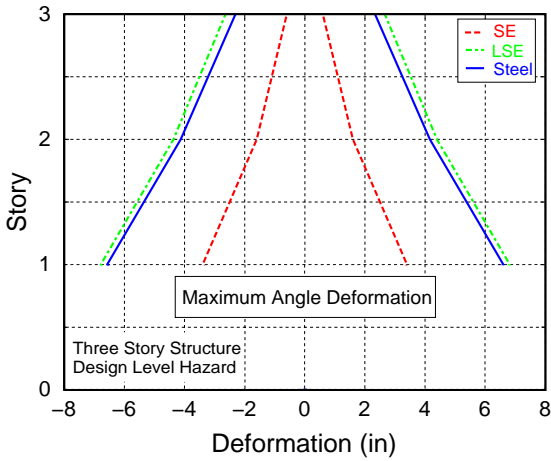


Figure 30.

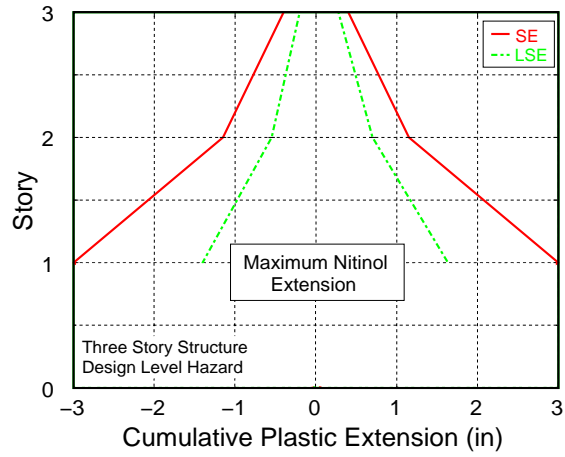


Figure 31.

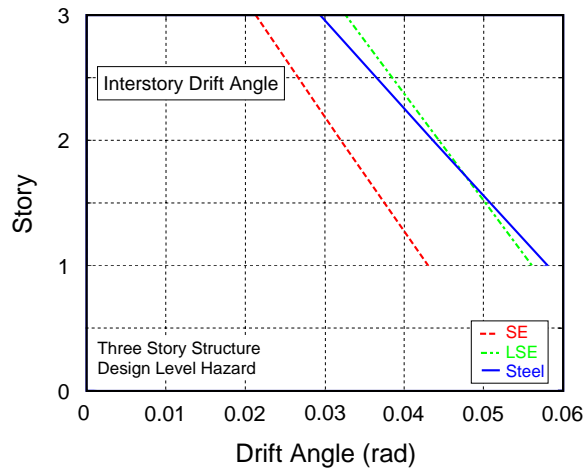
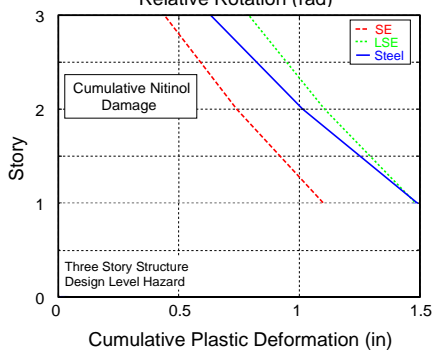
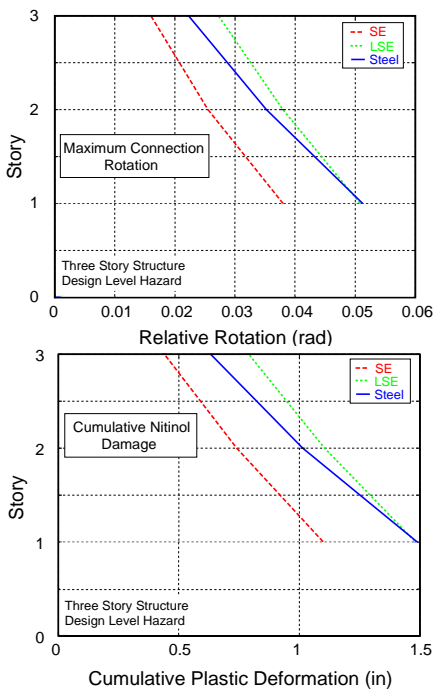


Figure 32.

B.1.c. Service Level Response: Pretension level

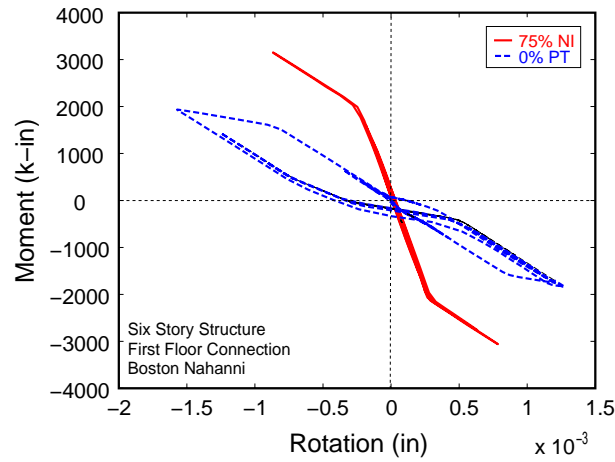


Figure 33.

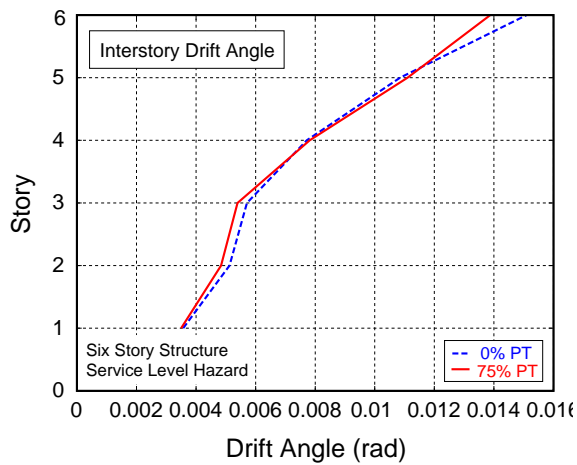


Figure 34.

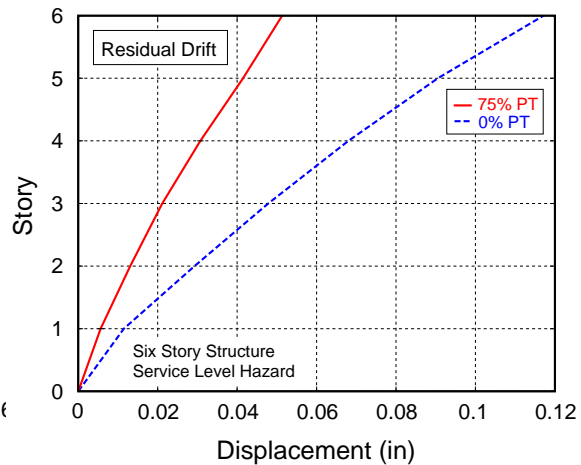


Figure 35.

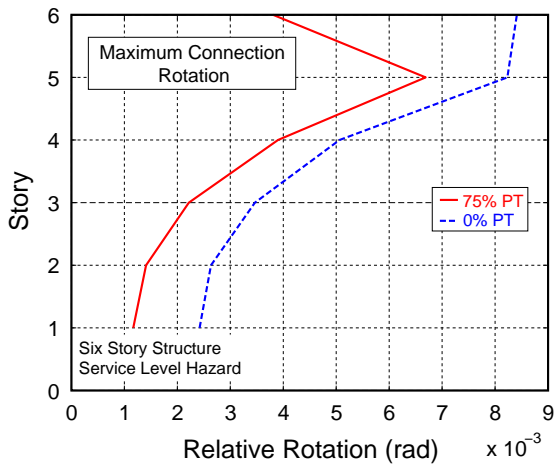


Figure 36.

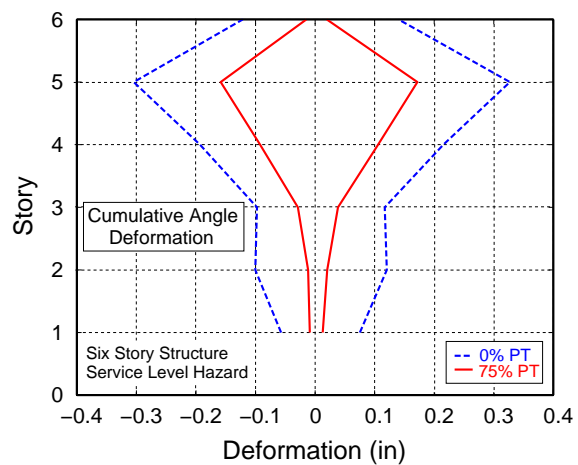


Figure 37.

B.1.d Design Level Response: Mild vs. Restoring Ratio

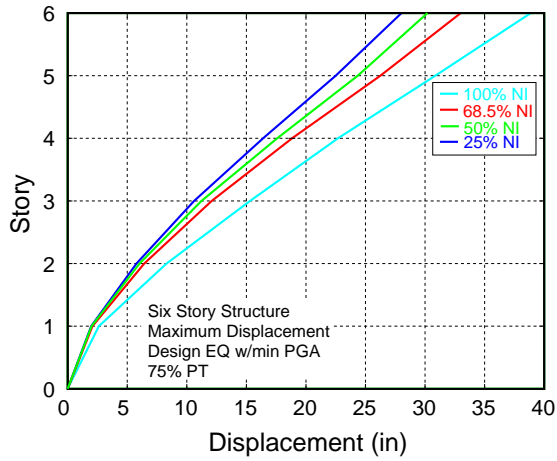


Figure 38.

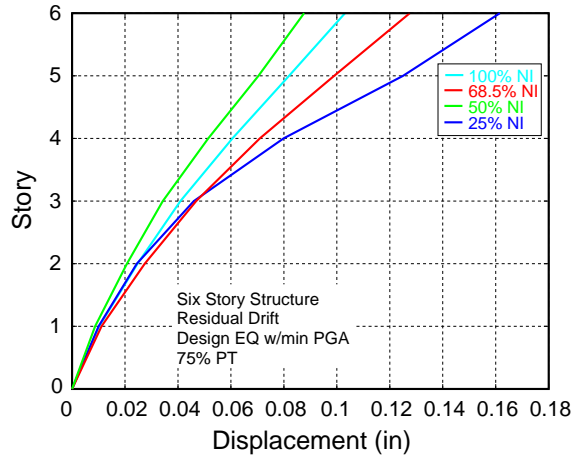


Figure 39.

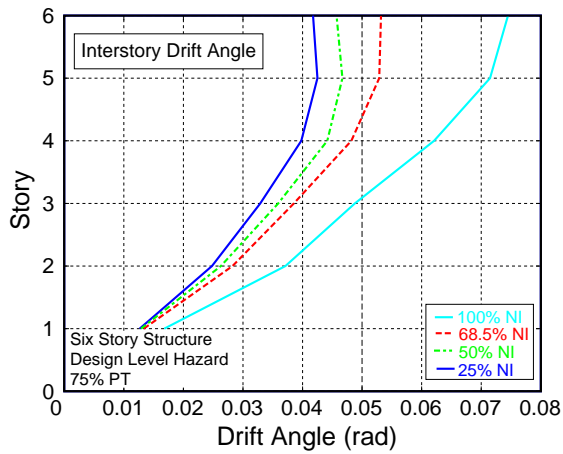


Figure 40.

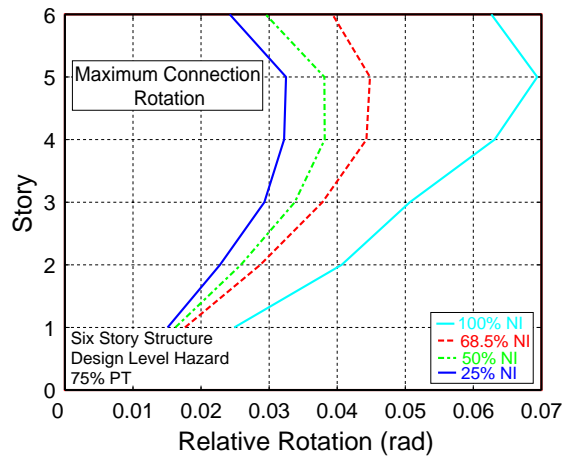


Figure 41.

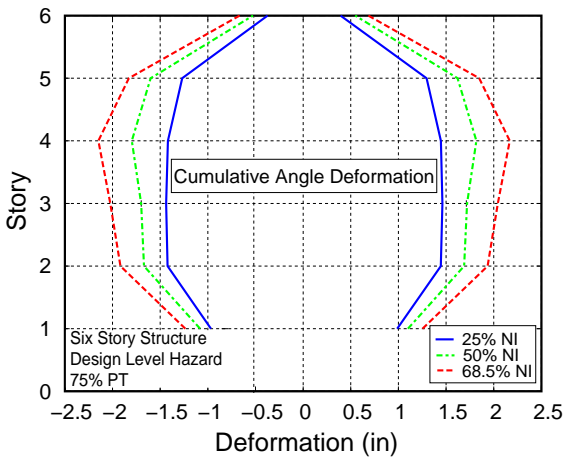


Figure 42.

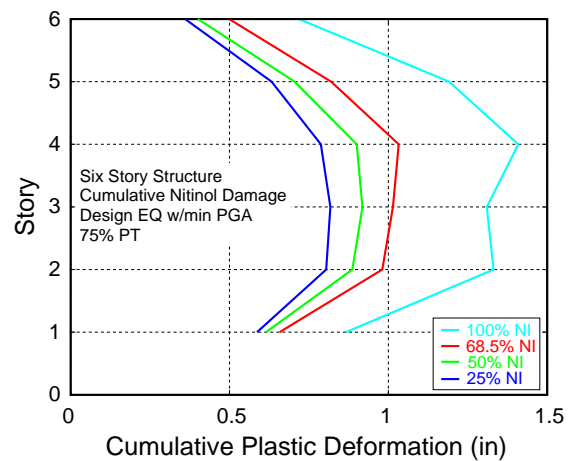


Figure 43.

B.1.e Improvement with increasing Post-tensioning Elements

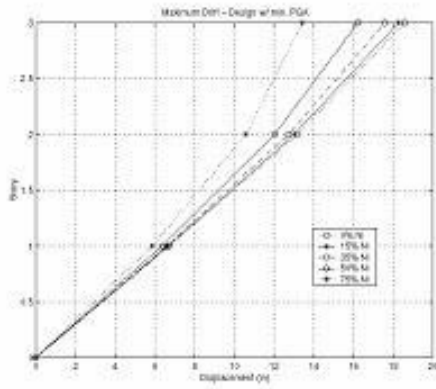


Figure 44.

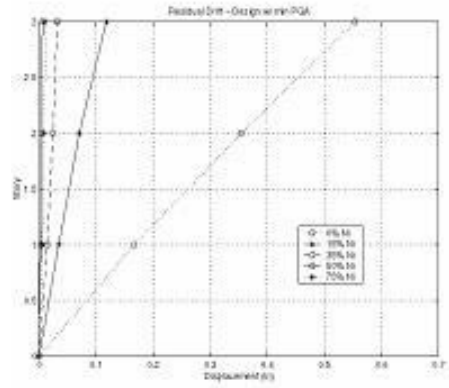


Figure 45.

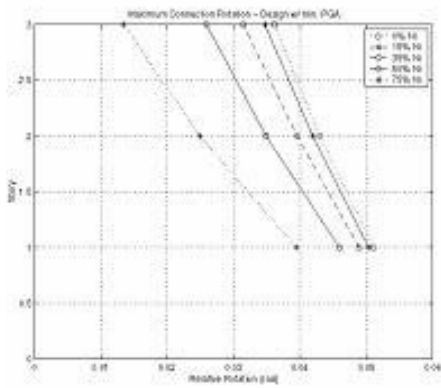


Figure 46.

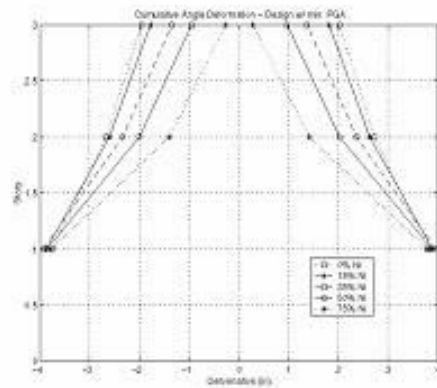


Figure 47.

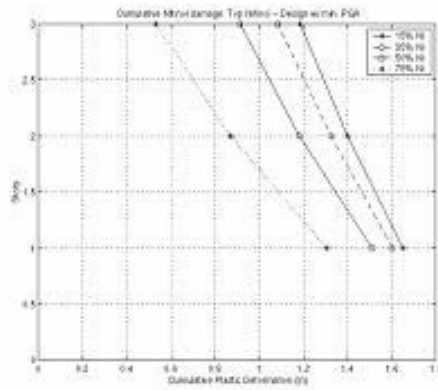


Figure 48.

B.2 Experimental Results

B.2.a Experimental Photographs



Figure 49.

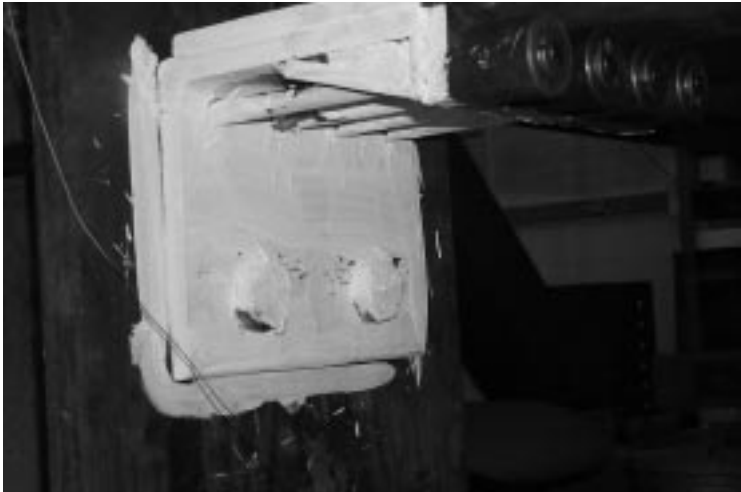


Figure 50.



Figure 51.



B.2.b Experimental Results

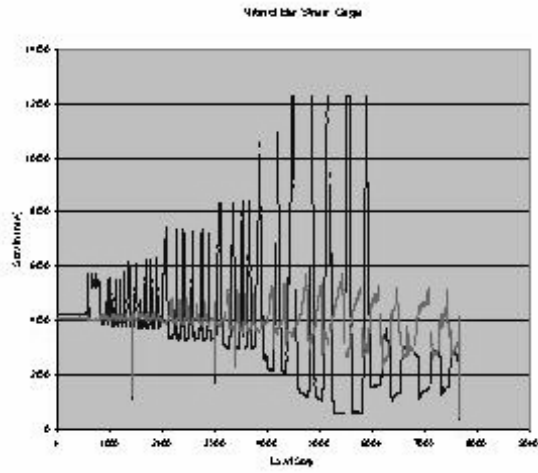


Figure 53.

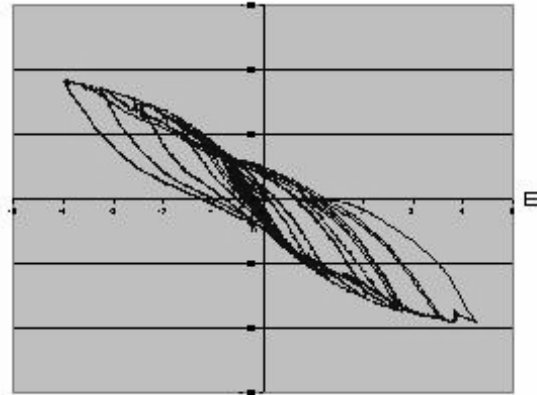


Figure 54.

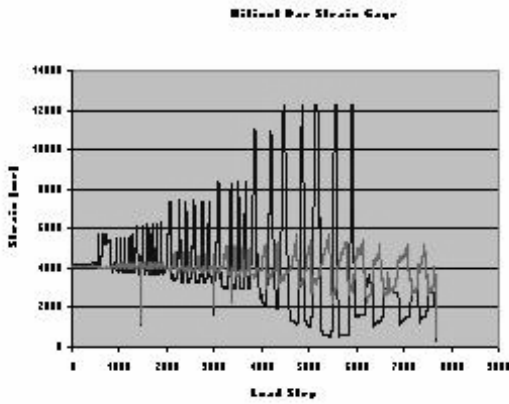


Figure 55.

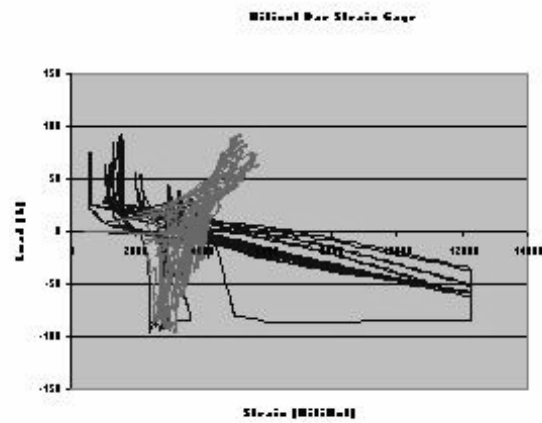


Figure 56.

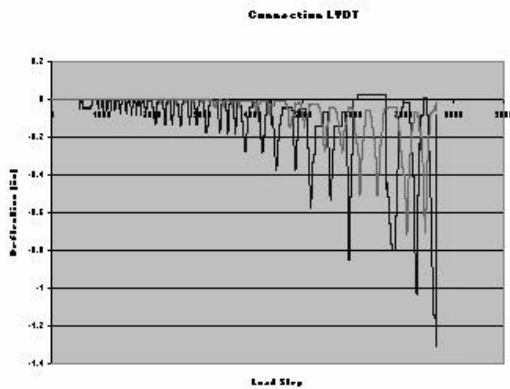


Figure 57.

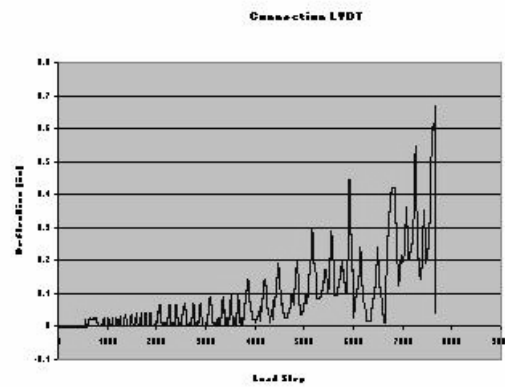


Figure 58.

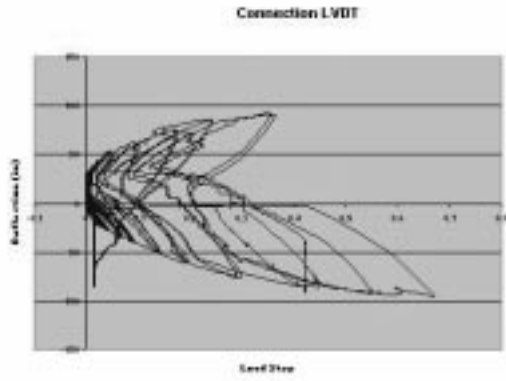


Figure 59.

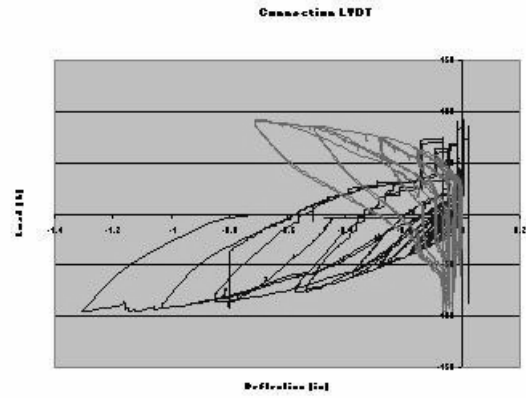


Figure 60.

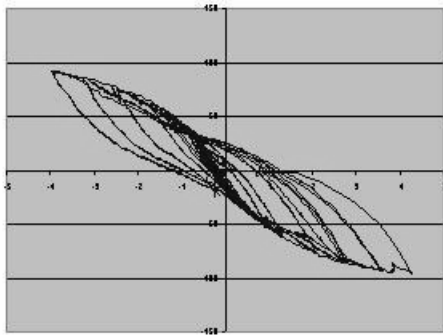


Figure 61.

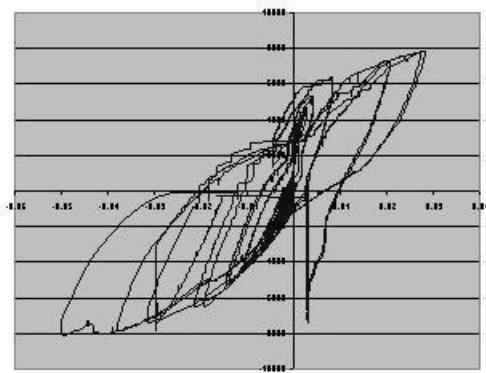


Figure 62.

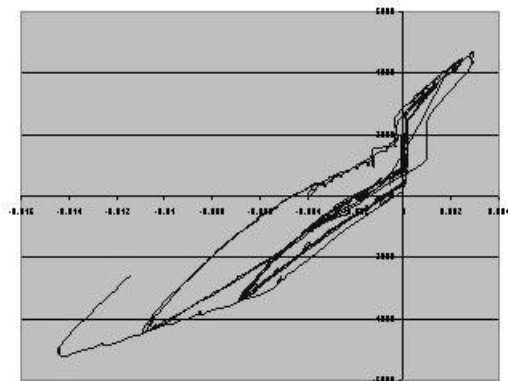


Figure 63.

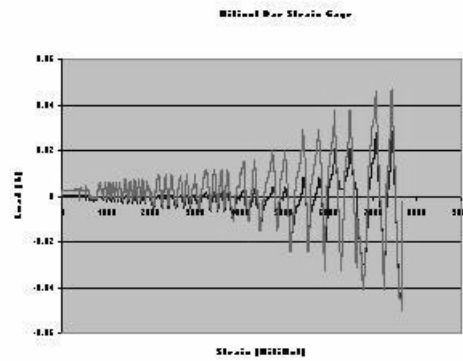


Figure 64.

